High-Resolution Imaging of the Active Galaxy PKS 0521–365 and its Optical Jet

R. FALOMO, Osservatorio Astronomico di Padova, Italy

1. Introduction

The galaxy hosting the radio source PKS 0521–365 is among the most remarkable extragalactic objects in the southern hemisphere. The source is at $z = 0.0554$ (Danziger *et al.* 1979) and exhibits a variety of nuclear and extranuclear phenomena. For these reasons 0521-365 was classified as N galaxy, Seyfert galaxy and BL Lac object.

A number of spectroscopic and imaging studies have been carried out (Danziger *et al.* 1979, 1985; Cayatte and Sol 1987; Boisson *et al.* 1989) showing the complex phenomenology of this object. The bright nucleus exhibits radio and optical flux variability together with strong polarization. Conspicuous variations were also found in the optical spectrum (Ulrich 1981; Scarpa *et al.* 1994) with large changes of equivalent widths of the broad lines. The broad-band energy distribution (see Pian *et al.* 1994) is dominated by a non-thermal component with a hard X-ray tail. This likely extends to higher energies as suggested by the recent detection of the source in the γ-rays (up to 100 MeV) by Fichtel *et al.* 1994.

Beside the nuclear activity the object shows also an extended emission region of gas of arc-like shape located up to 21 kpc from the nucleus (Boisson *et al.* 1989). The most remarkable feature is, however, the presence of a prominent optical jet (Danziger *et al.* 1979; Keel 1986; Macchetto *et al.* 1991) which extends for about 6″ to the NW from the nucleus.

The optical radiation from the jet is polarized indicating a non-thermal nature of the jet emission (Sparks *et al.* 1990). Radio mapping of the jet at 2 cm with VLA (Keel 1986) indicates the presence of a knotty structure similar to the jet in M87 with the brightest knot, at 1.7″ from the nucleus and elongated transverse to the jet direction.

High-resolution imaging of the galaxy surrounding 0521–365 and of its close environment is clearly an important tool to investigate the relationship between the activity and the host galaxy. In this paper we present the results obtained from high quality images for this source, obtained during a programme aimed at studying the properties of the environment of a sample of BL Lac objects.

2. Observations and Data Analysis

The observations were obtained on 5–6 January 1994 using the ESO NTT operated via remote control from Garching. Conditions were photometric and seeing was very good (FWHM < 0.7 arcsec) which favoured the use of SUSI to image the close environment of some objects.

The first night we obtained two images (2 and 15 minutes exposure) in the R filter, and a CCD (TK 1024) with 24 μm pixel size corresponding to 0.13 arcsec on the sky and seeing of 0.7″. One additional 15-minute exposure was secured the second night with 0.5″ seeing. A small ellipticity ($\lesssim 0.04$) was present for stellar objects in all images. The relevant portion of the 0.5″ seeing SUSI image is

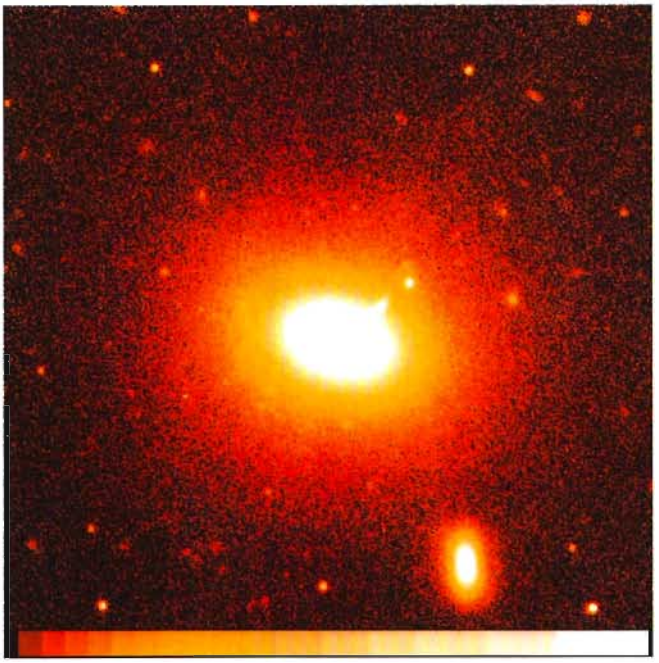

Figure 1: *The central portion (field $\sim 1' \times 1'$) of the NTT+SUSI image of PKS 0521–365 (R filter; 15-min exp.). North is at the top and east is to the left.*

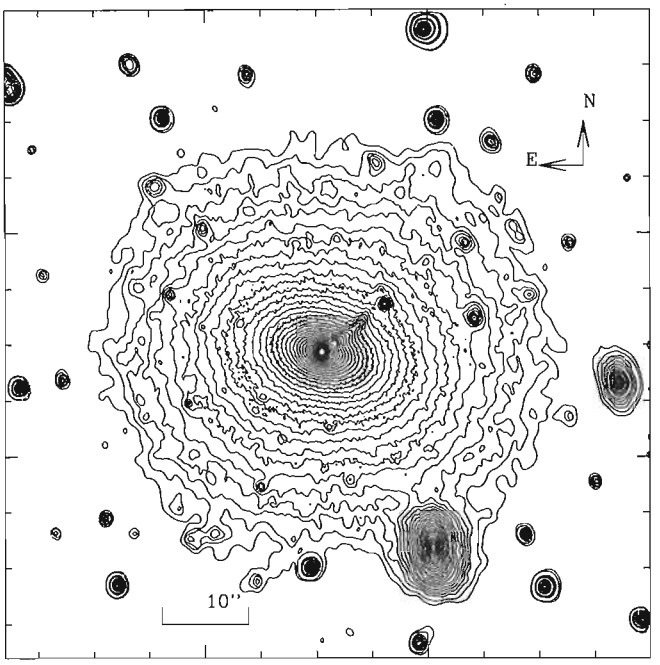

Figure 2: *A contour plot of the R-band image of the field centred on PKS 0521–365. The lowest isophote is $m_R = 25.5$ mag/arcsec^{-2} and spacing between isophotes is 0.25 mag.*

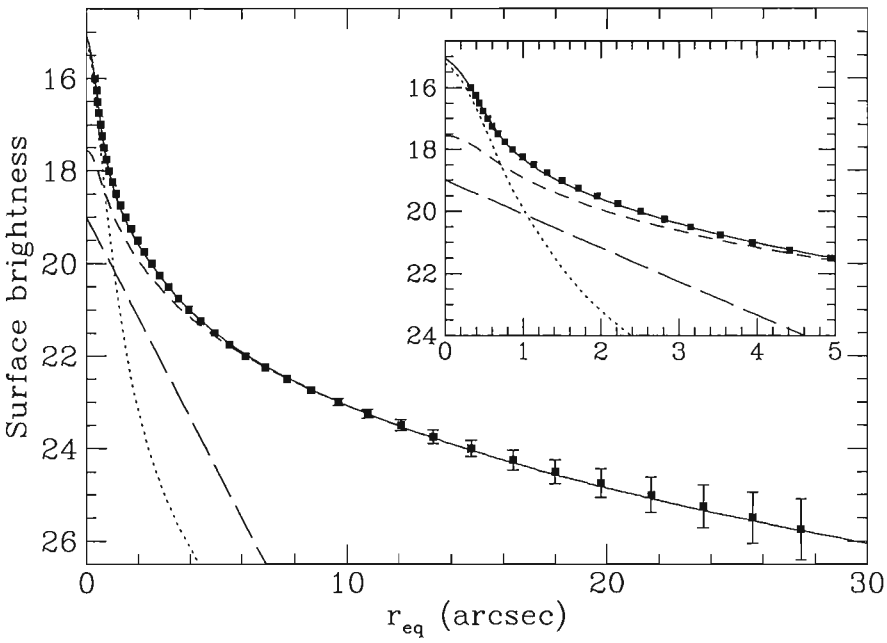

Figure 3: *The surface-brightness profile of PKS 0521–365 in the R-band filter (filled squares). The solid line is the sum of a PSF (dotted line) plus an elliptical $r^{1/4}$ law (short-dashed line) with r_e = 6.2 arcsec and an exponential disk with r_d = 1 arcsec (long-dashed line). The inset shows the inner region of the galaxy.*

reproduced in Figure 1 showing the host galaxy as well as the optical jet.

After standard reduction of the images (including cleaning of cosmic rays) we performed a surface photometry analysis using the numerical mapping package AIAP (Fasano 1994, in preparation). We computed isophotes down to μ_R = 25.75 mag/arcsec^{-2} (see Fig. 2) and then fitted them by an ellipse with free parameters. All the regions affected by fainter objects superposed to the galaxy were excluded by the fit using an interactive masking procedure. As a result of the analysis we obtain for each ellipse representing the isophote (with chosen spacing of 0.25 mag) the coordinates of the centre, the major axis, the position angle and the ellipticity. Moreover, the fourth cosine Fourier coefficient describing the deviations of the isophote from the pure ellipse is also provided. The analysis was performed for all three images giving consistent results but with the highest resolution image showing some more details. In the following we refer to the higher resolution image unless otherwise stated.

The surface photometry analysis may be used to study the galaxy morphology through the photometric and structural profiles (surface brightness, ellipticity, Fourier coefficients, ...). To study the brightness profile, we consider the surface brightness μ_R as a function of the equivalent radius r_{eq} ($r_{eq} = \sqrt{ab}$ where a and b are the semi-axes of the ellipse). The radial profile was modelled by a de Vaucouleurs ($r^{1/4}$) law, convolved with the point spread function (PSF), plus the contribution of the point source in the nucleus. In order to derive a reliable PSF that properly accounts for the core and wing components, we used unsaturated stars in the same frame as the target for modelling the core, and slightly saturated stars in other frames to derive the faint wing component.

In addition to the profile analysis, the mapping can be used to construct a model of the galaxy plus nuclear source to be subtracted from the original image in order to enhance the fine structures or the objects masked in the fitting procedure.

3. Results

The galaxy extends out to 30″ (at μ_R = 25 mag/arcsec^2) from the centre of the object and appears to be centred on the nucleus to within 0.1 arcsec. The isophotes beyond the region influenced by the central point source exhibit an ellipticity e = 0.3 and position angle PA = 75°. In the external regions ($r \gtrsim 10''$)

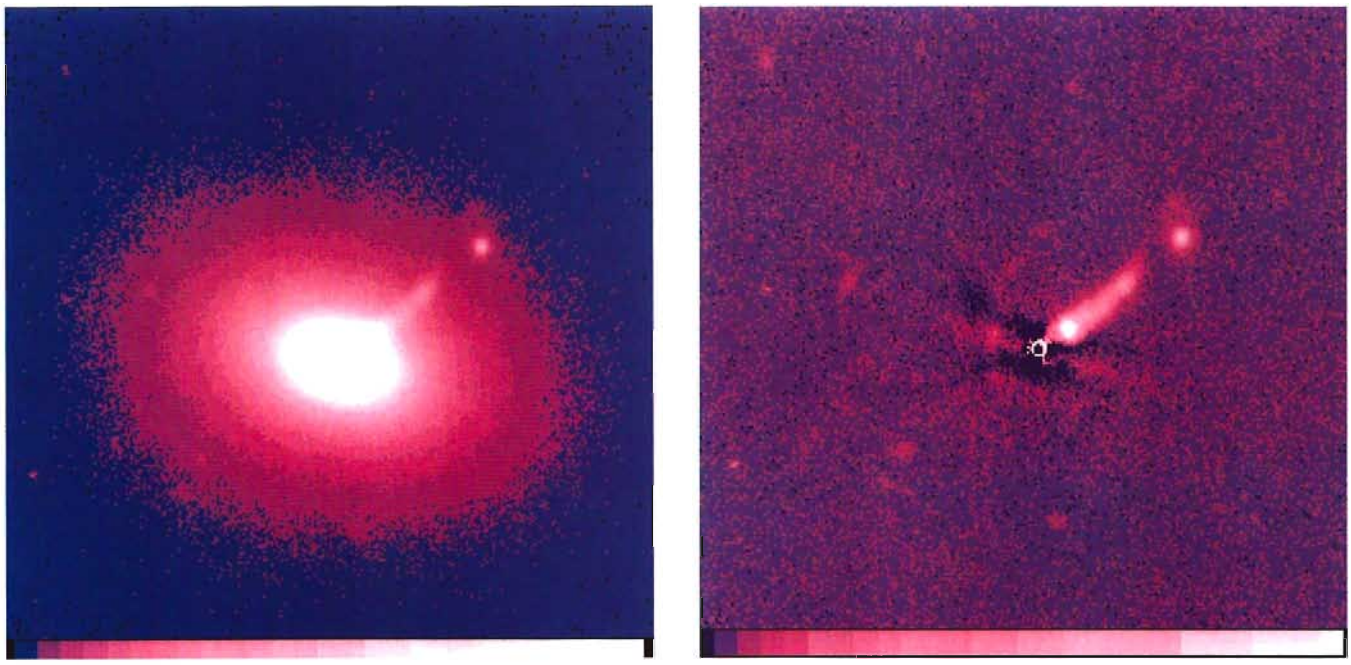

Figure 4: *The optical jet of PKS 0521–365 as imaged by NTT + SUSI in the R filter with 0.5 arcsec seeing before (left) and after (right) the subtraction of a model of the host galaxy plus nucleus. Note the knotty structure of the jet and its curvature. The field shown is 30″ × 30″.*

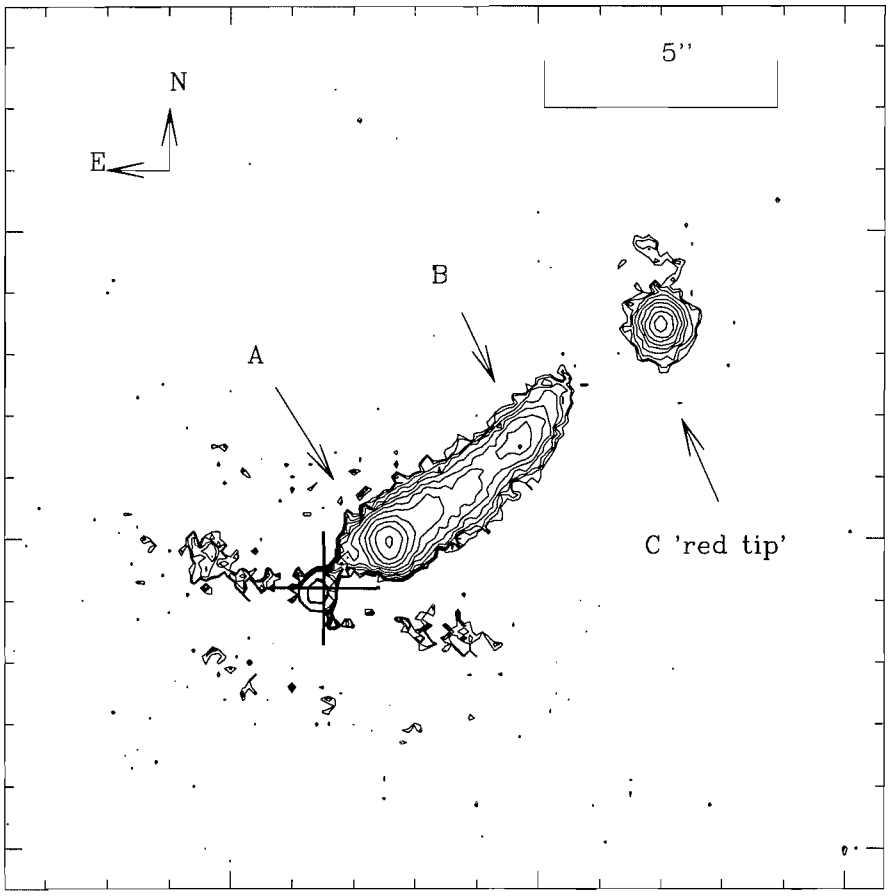

Figure 5: *Contour plot of the jet of PKS 0521–365 in the R band. The big cross represents the centre of the galaxy as derived from the surface-photometry analysis. Objects A and B are the primary and secondary knot in the jet. The nature of object C is unclear (see text).*

a slightly decreasing ellipticity is found. The brightness profile (see Fig. 3) is generally well described by the $r^{1/4}$ de Vaucouleurs law with r_e = 6.2″ plus a point source over the whole range, but around $r \sim$ 1.5″ there is an excess of emission with respect to the model. To account for this excess we add an exponential component which may represent the contribution of a faint disk to the inner part of the galaxy. The fit is substantially improved with a significant decreasing of the χ^2. The presence of a disk component is also suggested by a positive Fourier coefficient in the region between 1 and 4 arcsec. The best decomposition of the profile is thus obtained with a small exponential disk of characteristic radius r_d = 1″ and integrated magnitude 17.0. The magnitude of the galaxy derived by the model, including the bulge and the small disk, and integrated down to μ_R = 25.5 mag/arcsec^{-2} is m_R = 14.65, while the point source in the nucleus has a magnitude m_R = 16.0.

Assuming H_o = 50 km s^{-1} Mpc^{-1} and q_o = 0, the galactic extinction A_R = 0.15 and K-correction of 0.07, we found the absolute magnitude of the galaxy is M_R = –23.2, that corresponds to M_V = –22.4 (if V – R = 0.8), which is typical for galaxies hosting BL Lac objects. The effective radius is r_e = 9.2 kpc.

To study the optical jet, we have subtracted a model of the galaxy plus the nuclear source to the original image. This is an effective way of enhancing fine structures and it has been discussed in a recent issue of *The Messenger* (Reduzzi *et al.* 1994).

In Figure 4 both the original and the model-subtracted image of the 30″ × 30″ arcsec^2 around the nucleus are shown. The jet is clearly apparent together with the bright knot at 1.65″ and the object (known as the 'red tip') at 9″ from the nucleus in the direction of the jet.

In Figure 5 we report a contour plot of the jet with the main structures labelled. Figure 6 shows the intensity profile along the jet obtained averaging a strip of 1.3″ across the jet. The jet is clearly bent with upward concavity. The curvature radius of the jet is ∼ 80″. The whole jet (excluding the knot C) has an integrated magnitude $m_R(jet)$ = 19.3. The bright knot (A) which is 1.65″ (PA = 302°) from the nucleus (big cross) is resolved and elongated along the direction approximately perpendicular to the jet. Its magnitude is m_R(A) = 19.9. There is a secondary knot (B) at 5.0″ from the nucleus (PA = 308°) with a magnitude of ∼ 21.5. Finally the 'red tip' (C) at 9.0″and m_R(C) = 21.4 is also resolved indicating that it is not a galactic star.

4. Discussion

The analysis of the high-resolution images of PKS 0521–365 have allowed to study the optical properties of the host galaxy and of the optical jet. We found

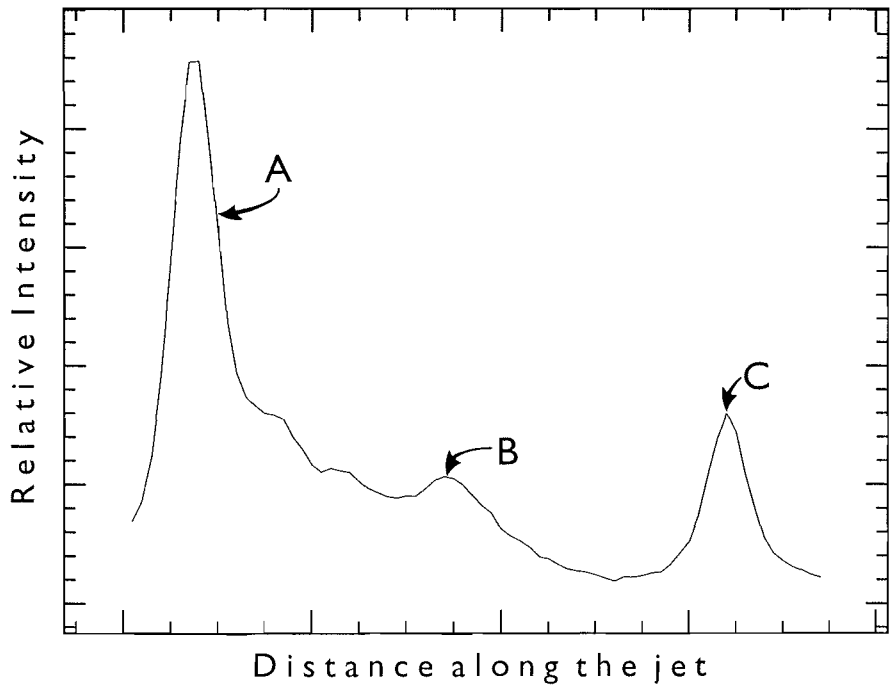

Figure 6: *Relative intensity along the jet obtained averaging the signal over a strip 1.3″ wide. Each large tick in the abscissa corresponds to 2.6 arcsec.*

the host galaxy to be a giant elliptical in agreement with previous studies but with probably a faint stellar disk. A similar feature was also found in the galaxy hosting the BL Lac PKS 0548–32 and may be not uncommon in early-type galaxies (see e.g. Scorza 1992). Its relation with the active nucleus (e.g. by accretion events) needs, however, a complete study for a larger sample of objects.

The optical jet is markedly knotty and resembles that of M 87 although it is more than a factor of 2 intrinsically brighter in the R band (cf. Biretta *et al.* 1991). Also the projected length of the jet (10 kpc) is much larger than that ($\sim$ 2 kpc) observed in M 87. The presence of the secondary peak (B) was suggested by the FOC image obtained with HST before the introduction of COSTAR and is well detected here. The decreasing optical intensity along the jet follows a behaviour very similar to that observed at 2 cm by Keel (1986).

Although the feature (C) is resolved, it remains unclear whether it is associated with the jet in some way or whether it is just a projected object. The lack of radio emission and of optical polarization favours the hypothesis that it is a projected faint galaxy. The centre of the 'red tip' is however very closely aligned with the bright knot and the centre of the galaxy.

Acknowledgement

I whish to thank G. Fasano for his kind assistance in the use of the AIAP package.

References

Biretta, J.A., Stern, C.P., and Harris, D.E. 1991, *AJ*, **101**, 1632.
Boisson, C., Cayatte, V., Sol, H. 1989, *A&A*, **211**, 275.
Cayatte, V., and Sol, H. 1987, *A&A*, **171**, 25.
Danziger, I.J., Fosbury, R.A.E., Goss, W.M., and Ekers, R. D. 1979, *MNRAS*, **188**, 415.
Danziger, I.J., Shaver, P.A., Moorwood, A.F. M., Fosbury, R.A.E., Goss, W.M., and Ekers, R.D. 1985, *The Messenger*, **39**, 20.
Fichtel, C. E., et al. 1994, *ApJS*, in press.
Keel, W. C. 1986, *ApJ*, **302**, 296.
Macchetto, F., et al. 1991, *ApJ*, **369**, L55.
Pian, E., Falomo, R., Ghisellini, G., Maraschi, L., Sambruna, R.M., Scarpa, R. & Treves, A. 1994, *Ap.J*, submitted.
Reduzzi, L. *et al.*, 1994, *The Messenger*, **75**, 28.
Scarpa, R., Falomo, R., & Pian, E. 1994, *PASP*, submitted.
Scorza, C., 1992, ESO/EIPC Workshop, *Structure, Dynamics and Chemical Evolution of Elliptical Galaxies*, p. 115, Ed. I.J. Danziger *et al.*
Sparks, W. B., Miley, G. K., and Macchetto, F. 1990, *ApJ*, **361**, L41.
Ulrich, M. H. 1981, *A&A*, **103**, L1.

Molecular Hydrogen Observations Towards Herbig-Haro Objects

R. GREDEL, ESO-La Silla

1. Introduction

The small optical line emission nebulae known as Herbig-Haro (HH) objects have received considerable attention in recent years. This is because HH objects are associated with young stellar objects, and their study may give insight into the processes that occur during star formation. It is believed that during the formation of a low-mass star a collimated jet of material is produced that emerges with supersonic speeds. The formation of jets may help to remove angular momentum from the forming stars. In the interaction regions of the jets with the ambient interstellar medium, bow shocks are created where the bulk energy of the outflowing material is converted into thermal energy. Temperatures in the shocks are raised to 2000–3000 K.

In recent years, it became evident that HH objects are also prominent emitters of molecular hydrogen lines in the near-infrared. To our delight, the near-infrared emission offers new possibilities to study the processes that occur in the shocked gas. The ground state of H_2 has a multitude of vibration-rotation levels with excitation energies ranging from less than 1000 K to several 10,000 K. The lowest levels, with vibrational quantum number $v \leq 3$, can be collisionally excited in the shock-heated gas. This case is referred to as thermal excitation. Levels above $v > 3$ are too high in energy and are not excited.

Two alternative, non-thermal, excitation mechanisms have also been discussed in connection with HH flows. In many cases the shocks are fast enough to produce ultraviolet and X-ray photons. The radiation might fluorescently excite the electronic states of H_2, or lead to excitation of the electronic states via impact by the secondary electrons produced by the X-rays. The decay of the electronic states competes with the collisions to populate the vibrational levels in the ground state, and, in particular, it populates levels in $v > 3$. If the shock speeds become too high, the shocks are dissociative and H_2 is destroyed. Nevertheless, H_2 emission can still occur, because H_2 eventually re-forms in the post-shock region where the gas is cooling. Part of the energy that is released when two H atoms combine to form H_2 is converted into excitations of the vibrational levels, which also include $v > 3$.

It has been suggested that each of the non-thermal excitation scenarios described here is strong enough to lead to observable effects. Schwartz *et al.* (1987) have performed calculations for the specific case of HH 43. The authors considered excitations by ultraviolet Lyα photons and predicted the resulting near-infrared emission spectrum. They also obtained a low-resolution CVF spectrum which appeared to contain emission lines from $v > 3$. Wolfire & Königl (1991) discussed low-resolution CVF spectra obtained by Harvey *et al.* (1986) towards HH 1, and suggested that the H_2 emission is primarily excited by UV continuum fluorescence and by collisions in an UV and X-ray heated gas, rather than by collisions in a shock. And finally, Carr (1993) proposed that the weak emission towards HH 11 is caused by reforming molecules behind a fast dissociative shock. However, recent medium-resolution H_2 spectra of HH objects, obtained with IRSPEC, have cast new light on these interpretations.

2. IRSPEC Observations

IRSPEC, the ESO near-infrared spectrograph on the ESO 3.5-m New Technology Telescope (NTT), is an ideal instrument to obtain accurate spectroscopy in the 1–5 μm range. IRSPEC provides long-slit capabilities and a spectral res-